LUND UNIVERSITY

A Minimal Solution to Relative Pose with Unknown Focal Length and Radial Distortion

Jiang, Fangyuan; Kuang, Yubin; Solem, Jan Erik; Åström, Karl

Published in:
[Host publication title missing]

DOI:
10.1007/978-3-319-16808-1_30

2015

Link to publication

Citation for published version (APA):
Jiang, F., Kuang, Y., Solem, J. E., & Åström, K. (2015). A Minimal Solution to Relative Pose with Unknown Focal Length and Radial Distortion. In M. Brown, T.-J. Cham, & Y. Matsushita (Eds.), *[Host publication title missing]* (Vol. 9004, pp. 443-456). Springer. https://doi.org/10.1007/978-3-319-16808-1_30

Total number of authors:
4

General rights
Unless other specific re-use rights are stated the following general rights apply:
Copyright and moral rights for the publications made accessible in the public portal are retained by the authors and/or other copyright owners and it is a condition of accessing publications that users recognise and abide by the legal requirements associated with these rights.
• Users may download and print one copy of any publication from the public portal for the purpose of private study or research.
• You may not further distribute the material or use it for any profit-making activity or commercial gain
• You may freely distribute the URL identifying the publication in the public portal

Read more about Creative commons licenses: https://creativecommons.org/licenses/

Take down policy
If you believe that this document breaches copyright please contact us providing details, and we will remove access to the work immediately and investigate your claim.

LUND UNIVERSITY

PO Box 117
221 00 Lund
+46 46-222 00 00

Download date: 07. Dec. 2025

A Minimal Solution to Relative Pose with Unknown Focal Length and Radial Distortion

Fangyuan Jiang[1] Yubin Kuang[2] Jan Erik Solem[1,2] Kalle Åström[1]

[1]Centre for Mathematical Sciences, Lund University, Sweden
[2]Mapillary AB, Sweden

Abstract. In this paper, we study the minimal problem of estimating the essential matrix between two cameras with constant but unknown focal length and radial distortion. This problem is of both theoretical and practical interest and it has not been solved previously. We have derived a fast and stable polynomial solver based on Gröbner basis method. This solver enables simultaneous auto-calibration of focal length and radial distortion for cameras. For experiments, the numerical stability of the solver is demonstrated on synthetic data. We also evaluate on real images using either RANSAC or kernel voting. Compared with the standard minimal solver, which does not model the radial distortion, our proposed solver both finds a larger set of geometrically correct correspondences on distorted images and gives an accurate estimate of the radial distortion and focal length.

1 Introduction

Estimating the camera motions from the image matches is a fundamental problem in the geometric computer vision. It is also one of the essential components to the large-scale 3D reconstruction system, e.g. Photo Tourism [1]. However, as the wide-angle cameras, e.g. GoPro or the cameras with digital zoom become more common and popular, a lot of images captured are radially distorted. Without handling the distortion, it will have a non-negligible effect in the estimate of the essential matrix or fundamental matrix, since the epipolar constraints have to be set very loose in order to find enough correspondences, which might also increase the number of outliers. Besides, if the radially mis-aligned images are used in a Structure-from-Motion (SfM) pipeline, it can cause significant skewness [2]. So estimation of radial distortion is an important task in a reconstruction pipeline with images captured by distorted lens.

Early works on estimation of the radial distortion is usually done in an offline manner. One first calibrates the cameras, finds the focal length and the radial distortion parameter. The epipolar geometry is then estimated separately afterwards. This requires either the knowledge of the 3D points [3] or the extra calibration object or pattern [4]. However, these offline methods have a large drawback that one need to have the original camera lens at hand. If the images are from the archived collection, or downloaded from internet, then the offline calibration becomes impossible.

Fig. 1. An example of radially distorted image (Left) captured by a GoPro Hero3 camera and the undistorted image (right) using our method.

With the online estimation method, the calibration could be handled in a more general situations. The plumb line ideas [5–7] are based on the fact that a straight line is preserved under an ideal pinhole camera. Extra knowledge are required to tell which curves in the image are the projections of straight lines in the 3D scene. However, the real scene, e.g. natural scene does not always contain a straight lines. Even it does, recognition of such a line also needs some effort. Contrary to the plumb line methods, the other methods [2, 8–14] requires nothing but only the rigidity assumption of the scene and the point correspondences between the views. Due to the simple assumption and off-the-shelf matching algorithms, e.g. SIFT [15], these methods become very popular.

The minimal problems, which are defined as using the minimal point correspondences to estimate the epipolar geometry as well as the camera calibration, e.g. focal length or radial distortion, plays an important role in these methods. The solver to the minimal problems are particularly useful when equipped with RANSAC[16], leading to a robust estimation method. However, to solve the minimal problems, one usually needs to handle some complex algebraic constraints. One example is when estimating the fundamental matrix F, the determinant constraint on $\mathtt{F}$ gives a cubic polynomial equation, which is difficult to cope with. This is why the early methods, such as [2, 9] ignored this algebraic constraint, but solves a simpler system using more points than the minimal requirement. More specifically, in [2], a non-minimal algorithm is given to simultaneously estimate the fundamental matrix and the single radial distortion parameter. The division model it proposed for radial distortion is extensively used in the later works. In [9], the authors treated exactly the same problem as [2] but used a hidden-variable method on the polynomial equations. A kernel voting scheme is used instead of RANSAC to avoid the computation of undistorted image point in each iteration. Another work on non-minimal solver is [8], where a 4×4 radial fundamental matrix is proposed to model the bilinear relation between the lifted point in one view and the corresponding epipolar curve in the other view. A non-minimal 15 points algorithm is given. The drawback of these non-

minimal methods is that it usually requires more RANSAC iterations to find an outlier-free set, which will increase the time complexity of the algorithms.

Thanks to the recent progress in the Gröbner basis method [17], solving a polynomial system becomes feasible, fast and stable. More focus are attracted to solving the minimal problems. All these works [11, 18, 13, 19, 20, 14] are based on the minimal solvers. In [11], a minimal solver using eight point correspondences is given to estimate the fundamental matrix and the single radial distortion parameter for the uncalibrated case. In [18], two minimal problems are proposed. One is to estimate the essential matrix `E` and the same radial distortion assuming the two cameras are partially calibrated with known focal length f, the other is to estimate the fundamental matrix `F` and two different radial distortion parameters for two uncalibrated cameras. For the first problem, the trace constraint on `E` is used to reduce the problem to a minimal one. The exact rational arithmetic solvers are given for both problems in Maple, which is very slow and impractical. In [13], based on the efficient implementation of Gröbner basis computation in floating point arithmetic, two solvers, which are much faster, are proposed for the two minimal problems in [18]. In [14], the one-sided problems are studied, which is to estimate the radial distortion for one camera assuming the other is already known. Three minimal problems are solved regarding to the uncalibrated case using 8 points, the calibrated case with unknown focal length using 7 points and the calibrated case with known focal length using 6 points. In [19], absolute pose estimation problem with unknown focal length is considered by incorporating the radial distortion. A 4-point algorithm is given based on Gröbeer basis. In [20], simple concepts from linear algebra, instead of Gröbeer basis, are used that leads to a real-time solution to the same pose problem.

In this paper, we study the minimal problem of estimating the relative pose with both the focal length and the radial distortion unknown. This is a very general and useful setting when the images are captured by one camera model with distortion. Up to our knowledge, this still remains an unsolved problem in the area. Compared with the previous minimal problems, this is more difficult since when both focal length and radial distortion are unknown, the epipolar constraint on essential matrix `E` leads to a polynomial equation with higher degrees. Also estimating `E` generally requires more effort than estimating F as one need to incorporate extra constraint, e.g. trace constraint in the system. By using the division model in [2], we derive a parametrization and simplify the polynomial system using a linear elimination scheme. We then study the simplified polynomial system and verify the number of solutions. A fast and stable polynomial solver is developed to solve the system. With our solvers, one can use it with RANSAC or kernel voting, to find the estimate of camera motions, which could be served as the initialization for bundle adjustment.

2 Problem Formulation

In this section, we will first introduce the camera model and the model for radial distortion. We give a parametrization of the image point to incorporate

the unknown radial distortion. A polynomial equation system is then formulated using all the constraints given by the epipolar geometry. By linearly eliminating several variables, one can obtain a more simplified and compact formulation with fewer unknowns.

2.1 Camera and Radial Distortion Model

In our formulation, we use the pinhole camera model and assume a one-parameter division model as in [2]. The intrinsic matrix $\mathtt{K}$ of the camera is defined as

$$\mathtt{K} = \begin{bmatrix} f & s & p_x \\ 0 & \gamma f & p_y \\ 0 & 0 & 1 \end{bmatrix} \tag{1}$$

where f is the focal length of the camera, For most cameras, the pixels are square and there is no skew, so we could safely assume the skew s is zero and the aspect ratio γ takes the unity. The principal point given by (p_x, p_y) is usually at the centre of the image, i.e. $(0, 0)$. So by the above assumptions, we could reparametrize $\mathtt{K}$ using only one variable as

$$\mathtt{K} = \begin{bmatrix} 1 & 0 & 0 \\ 0 & 1 & 0 \\ 0 & 0 & w \end{bmatrix} \tag{2}$$

where $w = 1/f$. Note this can be done since K is only defined up to a scale. If we denote the inhomogeneous coordinates of undistorted image point as $\mathbf{x}_u = (x_u, y_u)^T$ and the radially distorted image point as $\mathbf{x}_d = (x_d, y_d)^T$, then the relation between $\mathbf{x}_d$ and $\mathbf{x}_p$ is given by the division model as

$$\mathbf{x}_u = \frac{1}{1 + \lambda \|\mathbf{x}_d\|^2} \mathbf{x}_d \tag{3}$$

where λ is the distortion coefficient and $\|\mathbf{x}_d\|$ is the distance from $\mathbf{x}_d$ to the centre of distortion. Here we assume the center of distortion is known and at the center of the image.

If we use the homogeneous coordinates as $\mathbf{p}_u = (x_u, y_u, 1)^T$, $\mathbf{p}_d = (x_d, y_d, 1)^T$ and $r_d = \|\mathbf{x_d}\|$, then (3) can be written as

$$\begin{bmatrix} x_u \\ y_u \\ 1 \end{bmatrix} \sim \begin{bmatrix} x_d \\ y_d \\ 1 + \lambda r_d^2 \end{bmatrix} = \begin{bmatrix} x_d \\ y_d \\ 1 \end{bmatrix} + \lambda \begin{bmatrix} 0 \\ 0 \\ r_d^2 \end{bmatrix} \tag{4}$$

which is equivalently

$$\mathbf{p}_u \sim \mathbf{p}_d + \lambda \mathbf{z} \tag{5}$$

where $\mathbf{z} = (0, 0, r_d^2)^T$ is known since $\mathbf{x}_d$ is given. In some cases, we need the normalized image point $\mathbf{p}_n$, which can be represented as

$$\mathbf{p}_n \sim \mathtt{K}^{-1}\mathbf{p}_u \tag{6}$$

It is well known [21] that for two calibrated cameras, the essential matrix $\mathtt{E}$ has 5 degrees of freedom. For two cameras with constant but unknown focal length f and radial distortion λ, the degree of freedom is in total 7. In two-view geometry, each point correspondence gives one constraint. Thus, the minimal problem of auto-calibration with unknown focal length and radial distortion needs 7 correspondences.

2.2 Parametrization and Formulation

We present in the following the parameterization and the problem formulation based the epipolar constraints and the constraints on essential matrix $\mathtt{E}$.

Given n point correspondences $\{(\mathbf{p}_{u_i}, \mathbf{p}'_{u_i}), i = 1, 2, ..., n\}$ of the undistorted image points, the epipolar constraints using fundamental matrix $\mathtt{F}$ are given by

$$\mathbf{p}_{u_i}^T(\lambda)\ \mathtt{F}\ \mathbf{p}'_{u_i}(\lambda) = 0, \quad i = 1, \ldots, n. \tag{7}$$

where $\mathbf{p}_u(\lambda)$ is parametrized using (5). Using the normalized image points $\mathbf{p}_{n_i} \sim \mathtt{K}\mathbf{p}_{u_i}$, the epipolar constraint can also be expressed using the essential matrix $\mathtt{E}$ as

$$\mathbf{p}_{n_i}^T(\lambda, w)\ \mathtt{E}\ \mathbf{p}'_{n_i}(\lambda, w) = 0, \quad i = 1, \ldots, n. \tag{8}$$

In our method, instead of directly parametrizing the essential matrix $\mathtt{E}$, here we parametrize on $\mathtt{F}$ and solve for $\mathtt{E}$ implicitly. The reason is that using the constraint in (7) instead of (8) will get rid of the parameter w of the focal length, this gives much simpler equations and will lead to a linear elimination strategy as we will show in next section. The fundamental matrix $\mathtt{F}$ is parametrized as

$$\mathtt{F} = \begin{bmatrix} f_1 & f_4 & f_7 \\ f_2 & f_5 & f_8 \\ f_3 & f_6 & f_9 \end{bmatrix}. \tag{9}$$

where the last element f_9 is set to be one to fix the scale. Then from the relation $\mathtt{E} = \mathtt{K}^T\mathtt{F}\mathtt{K}'$ where $\mathtt{K}' = \mathtt{K}$ in our case, the essential matrix $\mathtt{E}$ is parametrized using calibration matrix $\mathtt{K}$ in (2) as

$$\mathtt{E} = \mathtt{K}^T\mathtt{F}\mathtt{K}' = \begin{bmatrix} 1 & 0 & 0 \\ 0 & 1 & 0 \\ 0 & 0 & w \end{bmatrix}^T \begin{bmatrix} f_1 & f_4 & f_7 \\ f_2 & f_5 & f_8 \\ f_3 & f_6 & 1 \end{bmatrix} \begin{bmatrix} 1 & 0 & 0 \\ 0 & 1 & 0 \\ 0 & 0 & w \end{bmatrix} = \begin{bmatrix} f_1 & f_4 & wf_7 \\ f_2 & f_5 & wf_8 \\ wf_3 & wf_6 & w^2 \end{bmatrix}. \tag{10}$$

On the other hand, the singularity of the essential matrix $\mathtt{E}$ is enforced as:

$$\det(\mathtt{E}) = 0. \tag{11}$$

along with the trace condition such that the two singular values are equal:

$$2(\mathtt{E}\mathtt{E}^T)\mathtt{E} - \mathrm{trace}(\mathtt{E}\mathtt{E}^T)\mathtt{E} = 0. \tag{12}$$

Inserting (10) into (11) and (12), together with the point equations (7), we formulate the problem as solving a polynomial equation system. The polynomial system contains 17 equations in 9 unknowns, namely, $\{f_1, f_2, ..., f_8, \lambda, w\}$.

2.3 Eliminating Variables

Let us look at the first seven equations given by the point correspondences in (7), or equivalently

$$\begin{bmatrix} x_d \\ y_d \\ 1+\lambda r_d^2 \end{bmatrix}^T \begin{bmatrix} f_1 & f_4 & f_7 \\ f_2 & f_5 & f_8 \\ f_3 & f_6 & 1 \end{bmatrix} \begin{bmatrix} x'_d \\ y'_d \\ 1+\lambda r_d^2 \end{bmatrix} = 0, \tag{13}$$

by expanding the above multiplication and stack all the seven equations, one can reach the following linear system

$$\mathtt{A}\mathbf{x} = 0, \tag{14}$$

where $\mathtt{A}$ is a 7×15 coefficient matrix and $\mathbf{x} = (\lambda^2, \lambda f_3, \lambda f_6, \lambda f_7, \lambda f_8, f_1, \ldots, f_8, \lambda, 1)$ is a vector containing the unknown monomials. After applying the Gaussian elimination on (14), one can linearly eliminate 7 unknown monomials by expressing those in terms of the remaining 8 unknown monomials (include the constant 1). Since f_1, f_2, f_4, f_5 appear only in the linear terms in (13), so it is natural to eliminate those four variables. Besides, we also choose to eliminate $f_3, \lambda f_3$ and λ^2. This choice of eliminating variable will simplify the system as we will show. Now the eliminating monomials $\{f_1, f_2, f_3, f_4, f_5, \lambda f_3, \lambda^2\}$ can be represented as a linear combination of the remaining monomials, namely $\{\lambda f_6, \lambda f_7, \lambda f_8, f_6, f_7, f_8, \lambda\}$, or equivalently, each can are expressed as a quadratic function on unknown variables $\{f_6, f_7, f_8, \lambda\}$. For $f_1, f_2, \ldots, f_5$, we have

$$f_i = h_i(f_6, f_7, f_8, \lambda), \quad i = 1, 2, 3, 4, 5 \tag{15}$$

For λf_3 and λ^2, we have

$$\lambda f_3 = h_6(f_6, f_7, f_8, \lambda) \tag{16}$$

$$\lambda^2 = h_7(f_6, f_7, f_8, \lambda) \tag{17}$$

One can further eliminate f_3 in (16) by replacing it with $h_3(f_6, f_7, f_8, \lambda)$ as

$$\lambda h_3(f_6, f_7, f_8, \lambda) - h_6(f_6, f_7, f_8, \lambda) = 0 \tag{18}$$

So now one can substitute f_i in (10) with $h_i(f_6, f_7, f_8, \lambda)$ for $i = 1, 2, \ldots, 5$ and insert it into (11) and (12). Together with (17) and (18), we would obtain a

well-defined system of 12 polynomial equations (Note the trace constraint (12) leads to 9 equations) with 5 unknowns $\{f_6, f_7, f_8, \lambda, w\}$. The equations are of degree at most 9.

Solving such a polynomial system is certainly a non-trivial task. It is a more complicated system compared with the previous work. The formulation in [11] for uncalibrated case gives 3 equations with 3 unknowns, the degree of which is 5. The polynomial system in [14] for calibrated case, assuming the radial distortion and focal length for one view is already known, contains 11 equations with 4 unknowns, the degree of which is 5 or 6. With the recent progress in Gröbner basis method, we will show in the next section that it is possible to find a fast and stable solver for our minimal problem.

3 Polynomial Solvers

In this section, we will focus on the polynomial system we derived in the previous section and aims at finding a fast and stable solver based on the Gröbner Basis method. We will first give a brief review of the Gröbner Basis method.

3.1 Review of Gröbner Basis Method

We are aiming at solving a polynomial equation system in the following form

$$h_1(x) = 0, h_2(x) = 0, \ldots, h_m(x) = 0 \tag{19}$$

where $H = \{h_1(x), \ldots, h_m(x) \,|\, h_i \in \mathbb{C}[x_1, \ldots, x_n]\}$ are polynomials in n variables over the field $\mathbb{C}$ of the complex numbers. Using the notation in the algebraic geometry [22, 23], we consider the ideal I generated by the the polynomials $H = \{h_1(x), \ldots, h_m(x)\}$ defined by

$$I = \{\sum_{i=1}^{m} p_i h_i \,|\, p_i \in \mathbb{C}[x_1, \ldots, x_n],\ h_i \in H\} \tag{20}$$

In general, an ideal could be generated by different finite set of generators. However, all sets of generators share the same solutions. The idea of the Gröbner basis method for solving a polynomial equation system given by $\{h_i(x) = 0 | i = 1, \ldots, m\}$ is to find another set of generator $\{g_i(x) | i = 1, 2, \ldots, m\}$ that generates exactly the same ideal as $\{h_i(x)\}$ does, but $\{g_i(x) = 0\}$is a much simpler problem to solve. It turns out that reduced Gröbner basis w.r.t the lexicographic ordering is such a set of generator, which is usually simple or even trivial to solve.

However, to compute the complete set of Gröbner basis is usually very difficult due to the numerical stability. Also it requires a proper choice of the monomial order, e.g lexicographic order. Recent progress [17] in the Gröbner basis method provides a new action matrix method, which does not rely on finding the complete set of Gröbner basis, yet leads to a more stable algorithm. The key idea is to consider the quotient space $\mathbf{C}[\mathbf{x}]/I$, which is the space of all possible remainders under the multivariate division by the ideal I. By the theorem in [22],

if the equation system (19) has finite zeros, then $\mathbf{C}[\mathbf{x}]/I$ is finite-dimensional linear space, the dimension of which coincides with the number of zeros of (19).

Using this property, within the quotient space $\mathbf{C}[\mathbf{x}]/I$, the multiplication with a monomial x_k, known as action variable could be regarded as a linear map from $\mathbf{C}[\mathbf{x}]/I$ to itself. Due to the finite dimension of $\mathbf{C}[\mathbf{x}]/I$, this linear map can be represented using a matrix $\mathtt{M}_{x_k}$, called the action matrix. The eigenvalue of $\mathtt{M}_{x_k}$ directly gives the value of action variable x_k. The eigenvectors corresponds to the vector of monomials which are evaluated at the zeros of (19). More details are referred to [17].

3.2 A Polynomial Solver to Our Problem

We first study and explore the structure of the polynomial system generated from (11), (12), (17) and (18), one observation is that among the 12 equations, there are 4 equations has w as the common multiplier. To avoid the trivial and false solution $w = 0$, we divide w from all the 4 equations. The other observation is that, after we remove the common multiplier w, all the equations that contain w only contain the terms of even degrees, e.g. w^2, w^4, w^6. So we could simply replace w^2 with a new variable $z = w^2$. With these observations, we managed to simplify the system by decreasing the degree of the system from 9 to 7. Now we obtain a polynomial system contains one equation of degree 2, one of degree 3, two of degree 5, three of degree 6 and five of degree 7.

We then verify the number of solutions using some algebraic geometry tools. By generating the polynomial system with coefficients in $\mathbb{Z}_p$, and using Macaulay2 [24], we find that there are in general 68 solutions for this problem. Although the number of solution is relatively large, but we will show later in the experiments that most solutions in our problem are complex and thus could be simply removed.

To solve the system, we follow the method based on Gröbner basis in [17]. A redundant set of higher order polynomials, called *eliminating template*, are systematically generated from our initial polynomial equations by multiplying them with a set of monomials. With this step, one aim is to find a sufficient large set of monomials from which we could find the *basis*, i.e. a set of monomials. All the other monomials that are not included in *basis* could be represented as a linear combination of *basis*. The *permissible* monomials, which stay in itself after multiplication with an action monomial x_k will give us direct clues to construct the action matrix and further find the solution. Empirically we found that the following choice of multiplication monomials will generate a numerically stable solver. (i) the highest degree of monomials in those equations are up to 9 after the multiplication. (ii) the highest degree of those multiplication monomials are $\{4, 4, 4, 2, 4\}$ respectively for unknowns $\{f_6, f_7, f_8, w, \lambda\}$. After this multiplication step, the resulting *elimination template* contains 886 equations with 1011 monomials. Further attempt to reduce the size of the elimination template by decreasing the highest degree of multiplication monomials will affect the numerical stability as we tried.

We use a column-pivoting scheme [17] to select the basis with the improved numerical stability. The last 120 monomials is selected as the *permissible* set to construct the action matrix of size 68×68. Using the eigen-decomposition on the transpose of the action matrix, we could extract the solutions to our system from the resulting eigenvectors. Once we found the value of $\{f_6, f_7, f_8, w, \lambda\}$, the other unknowns on the fundamental matrix `F` could be found using (15). The essential matrix `E` is then solved from (10) as well.

4 Experiments

We test and validate our minimal solver on both synthetically generated image data and the real images. For synthetic image data, we validate the number of real solutions in general. We also test the numerical stability and the sensitivity to the noise. For the real images, we use both RANSAC and the kernel voting to obtain an accurate estimation of the essential matrix `E`, the radial distortion coefficient λ as well as the focal length f. We also compared with the standard 7-point algorithm of fundamental matrix estimation, which do not handle the radial distortion. As we will show later, taking the radial distortion into consideration, we will obtain more inliers using the RANSAC.

We implement the solvers in MATLAB. The average running time for our minimal solver is around 400ms(milliseconds). The timing are recorded on a Macbook Air with 8GB memory and 1.8 GHz i5 CPU. One could further reduce the running time by implementing the solver in C or C++. Other optimization strategy, e.g. [25, 26] is also a choice.

4.1 Synthetic Data

We generated random 3D points within a cube of width 1000 centered at the origin. Two cameras are placed to be around 1000 units away from the origin. The two cameras are roughly pointing to the origin with a random rotation. The translation between the two camera centers is around 300 units. The focal length for both cameras are randomly generated around 1000. The 2D image points are generated by projecting the 3D points into the image plane of size 1000×1000. Based on the division model in (3), we distort the image point with the distortion coefficient uniformly sampled from $[-0.5, 0]$. The radial distortion is specified w.r.t. the normalized image points in the range of $[-1, 1]$.

The first experiment is to test the numerical stability and validate the number of real solutions. For this experiment, we use the noise free image data. We randomly generated 1000 synthetic scenes in the way described above. For each scene, we run our minimal solver with 7 points and evaluate the relative error between the estimated value of radial distortion λ, the focal length f and their ground truth value. The relative errors for λ is defined as follows

$$e(\lambda_{est}) = \frac{|\lambda_{est} - \lambda_{gt}|}{|\lambda_{gt}|} \tag{21}$$

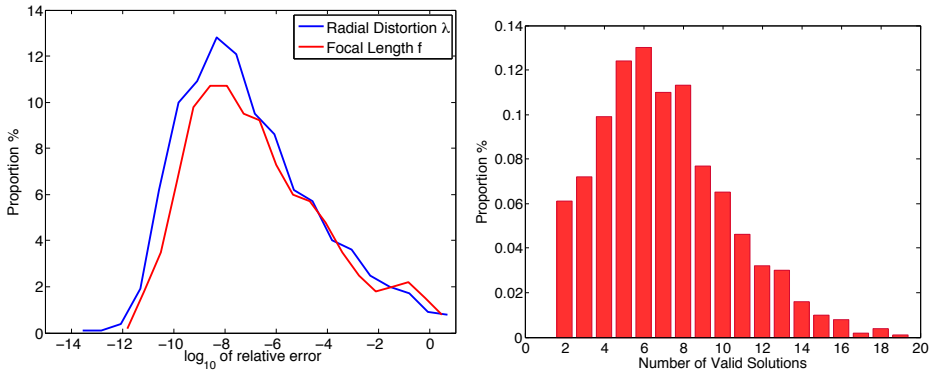

Fig. 2. Experiments on synthetic data without noise. Left: The distribution of log_{10} relative error of radial distortion λ and the focal length f. Right: The distribution of number of solutions

where λ_{est}, λ_{gt} are respectively the estimated and the ground truth value for the distortion. The relative error of f is defined in the similar way.

We plot the distribution of log_{10} of the relative error for λ and f in the left of Fig. 2, . We can see that our solver is generally very stable and give the accurate estimation of both λ and f. The medians of the log_{10} relative error are -7.49 for λ and -7.16 for f. The statistic of the number of valid solutions is also plotted in the right of Fig. 2. By valid solutions, we mean the real roots of the polynomial system. Although the system have in total 68 solutions, but most of them are of complex value and could be simply removed without the need of further validation. For most cases, there are 4 to 10 valid solutions.

The performance of our solver in the presence of noises is also tested. The image points are perturbed with Gaussian noise with different standard deviation $\tau = 0, 0.01, 0.1, 0.5, 1, 2$ respectively. We tried different radial distortion parameter $\lambda = -0.01, -0.1, -0.2, -0.5$ as well. In Fig. 3, we plot the box with the middle red line in the box as the median of the log_{10} relative error, the top and bottom edges of the box as the 25th and 75th percentiles. The red cross marks are the points lying beyond the 1.5 times the range. For noiseless data, our solver gives accurate estimates of radial distortion λ. We also noticed that the solver generally achieves more accurate estimates when the radial distortion is large. When noise level increases, the log_{10} relative errors also increase largely, to around 10^{-1}. This shows that one should use the solver on the repeatedly drawn minimal samples and combine it with either the kernel voting scheme or the RANSAC when the real data are contaminated with noise or outliers. Note we also tested the noise sensitivity for the estimation of focal length f and obtained quite similar box plot. Due to the space limitation, we will omit the resulting plot here.

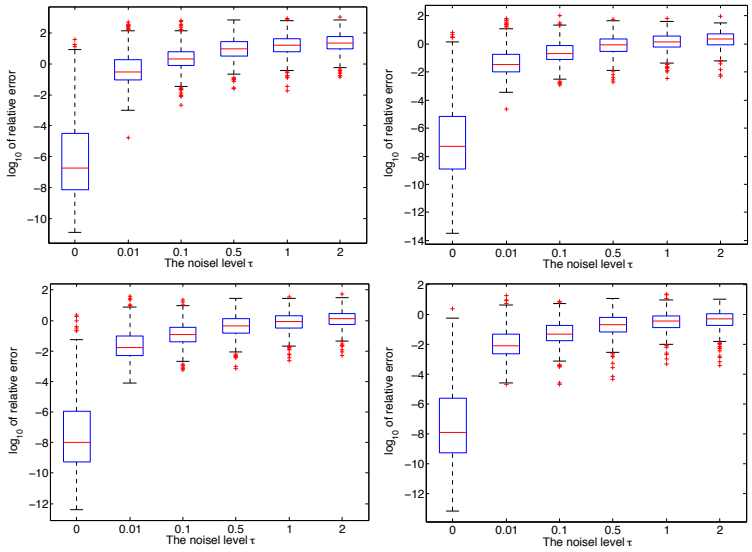

Fig. 3. Experiments on synthetic data with different noise levels. The log_{10} of relative error of λ for different radial distortion, where the ground truth are $\lambda = -0.01$ (Top left), $\lambda = -0.1$ (Top right), $\lambda = -0.2$ (Bottom left) and $\lambda = -0.5$ (Bottom right). See the text for detailed description.

4.2 Real Data

We further evaluate the proposed solver on real images. A GoPro Hero3 camera is used to capture the images with a significant radial distortion. The camera is calibrated with the fixed focal length, which serves as the ground truth for the algorithm evaluation. A set of 36 images are paired and used to test our solver. The SIFT features are extracted from all the images and matched between each pair using method in [15]. This produce a set of tentative matches which also contains outliers.

We first use the RANSAC algorithm equipped with our minimal solver as a subroutine to estimate the essential matrix $\mathtt{E}$, the focal length f and the radial distortion λ. In each RANSAC iteration, different minimal sets of point correspondences are randomly drawn and are fed into our solver. With the estimated $\mathtt{E}$, λ and f, we compute the distance to the epipolar line for each point and obtain an inlier set containing all the points with distance smaller than a threshold. The solution with the maximum inlier set gives the final estimation of $\mathtt{E}$, λ and f. The standard 7 point algorithm, which does not consider the radial distortion, serves as a baseline in RANSAC to estimate the fundamental matrix. Note we set the RANSAC iterations to be 1000 and the threshold of inliers to be 3 pixels for both methods in the experiment. From Fig. 4, our minimal solver obtains a substantially larger inlier set due to the explicit modeling of the radial distor-

tion. Quatitatively, our minimal solver gains average 49.37% increase w.r.t. the number of inliers compared with the standard 7 point solver on the image set.

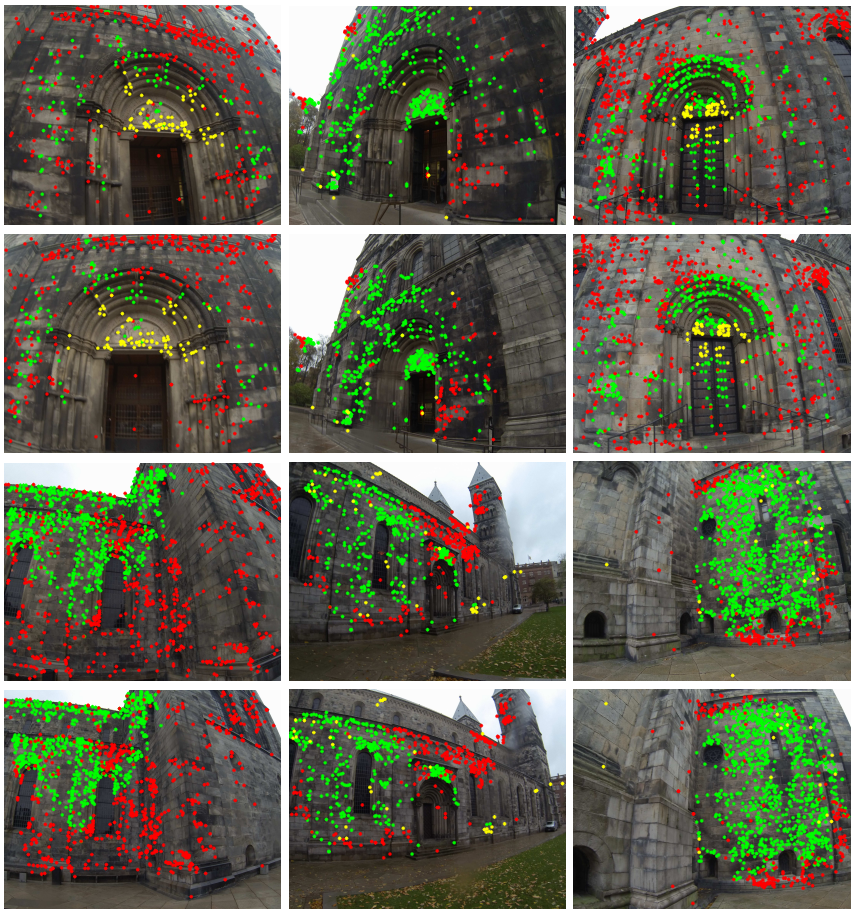

Fig. 4. Experiments on read data using RANSAC. The inlier set using different method are marked. The green star marks are inliers found by both methods. The red stars are the inliers only found using our method, The yellow starts are the inliers only found by standard 7 point solver. Note that the images are paired for the top two rows and bottom two rows.

We also use a kernel voting scheme to estimate the $\mathtt{E}$, λ and f. To avoid the computation of the undistorted image point and the fundamental matrix in each iteration of RANSAC, the kernel voting finds the estimate by fitting a kernel, e.g. Gaussian kernel to all the solutions one obtained from different random minimal samples. The success of the method is based on the observation that

the solved roots are all around the genuine root regardless of the noises. In this experiment, we randomly draw 1000 minimal set, solve them and keep all the real roots. Gaussian kernel with bandwidth $w = 0.02$ for radial distortion parameter λ and $w = 200$ for focal length f are fitted to all the solutions of λ and f. These bandwidths are reasonable choices considering that $\lambda \in [-1, 1]$ and $f \in [0, 2000]$. Then the peak is picked out as the final solution for λ and f respectively. From the distribution of real roots of λ and f in Fig. 5, we could easily see the peak, around which are the genuine solutions. The kernel voting gives an estimate of -0.28 for λ and 1793.4 for f, which are plotted as blue lines in the Fig. 5. Note we also plot the ground truth value of f, which is 1765.6, in the right part of Fig. 5 as a green line. It shows the estimate of f is very close to the ground truth. Note the Fig. 5 is the plot for only one of the image pairs. As we have tested, all the other image pair gives consistent estimate on λ and f and further validate the proposed solver.

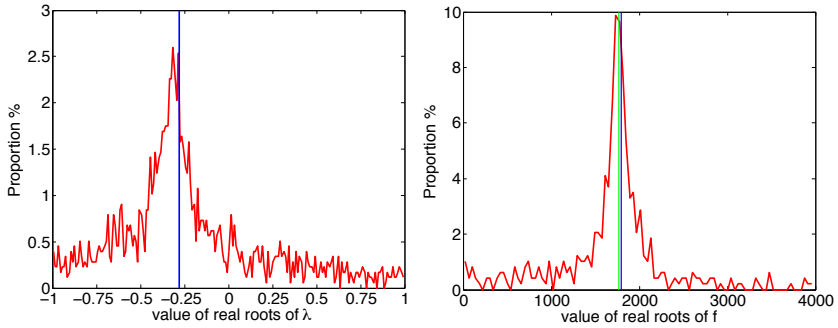

Fig. 5. Experiments on read data using kernel voting. The distribution of real roots (red curve) for radial distortion coefficient λ and focal length f are shown in the left and right figure respectively. The estimate of λ and f (blue line) as well as the ground truth of f (green line in the right figure) is also marked.

5 Conclusion

In this paper, we have given a fast and numerically stable solver for the minimal problem of estimating the relative pose with unknown focal length and radial distortion. We use a division model for radial distortion and derive a parametrization and formulate a polynomial system. After studying the polynomial system, we simplify it by variable elimination and use Gröbner basis method to derive a solver. We evaluate our solver on both the synthetic data and real images. The solver is shown to be numerically stable on synthetic data. With the RANSAC or kernel voting, the solver could be applied to real image data with noises and

outliers. It finds more point correspondences and gives accurate estimates on the relative pose, as well as focal length and radial distortion.

References

1. Snavely, N., Seitz, S.M., Szeliski, R.: Photo tourism: exploring photo collections in 3d. In: SIGGRAPH '06: ACM SIGGRAPH 2006 Papers, New York, NY, USA, ACM (2006) 835–846
2. Fitzgibbon, A.W.: Simultaneous linear estimation of multiple view geometry and lens distortion. In: Proc. of Computer Vision and Pattern Recognition Conference. (2001) 125–132
3. McGlone, J., Mikhail, E., Bethel, J., Mullen, R., for Photogrammetry, A.S., Sensing, R.: Manual of photogrammetry. American Society for Photogrammetry and Remote Sensing (2004)
4. Tsai, R.Y.: A versatile camera calibration technique for high-accuracy 3d machine vision metrology using off-the-shelf tv cameras and lenses. IEEE J. Rob. Autom. **3** (1987) 323–344
5. Devernay, F., Faugeras, O.D.: Straight lines have to be straight. Mach. Vis. Appl. **13** (2001) 14–24
6. Swaminathan, R., Nayar, S.K.: Nonmetric calibration of wide-angle lenses and polycameras. IEEE Trans. Pattern Anal. Mach. Intell. **22** (2000) 1172–1178
7. Kang, S.: Semiautomatic methods for recovering radial distortion parameters from a single image. Cambridge Research Laboratory technical report series. Digital, Cambridge Research Laboratory (1997)
8. Barreto, J., Daniilidis, K.: Fundamental matrix for cameras with radial distortion. In: IEEE International Conference on Computer Vision, Beijing, China (2005)
9. Li, H., Hartley, R.: A non-iterative method for correcting lens distortion from nine point correspondences. OMNIVIS 2005 (2005)
10. Stein, G.P.: Lens distortion calibration using point correspondences. In: CVPR. (1997) 602–608
11. Kukelova, Z., Pajdla, T.: A minimal solution to the autocalibration of radial distortion. In: In Proc. Conf. Computer Vision and Pattern Recognition. (2007)
12. Kukelova, Z., Pajdla, T.: A minimal solution to radial distortion autocalibration. Pattern Analysis and Machine Intelligence, IEEE Transactions on **33** (2011) 2410–2422
13. Kukelova, Z., Byröd, M., Josephson, K., Pajdla, T., Åström, K.: Fast and robust numerical solutions to minimal problems for cameras with radial distortion. Computer Vision and Image Understanding **114** (2010) 234–244
14. Kuang, Y., Solem, J.E., Kahl, F., Åström, K.: Minimal solvers for relative pose with a single unknown radial distortion. In: Proc. Conf. Computer Vision and Pattern Recognition. (2014)
15. Lowe, D.G.: Distinctive image features from scale-invariant keypoints. Int. Journal of Computer Vision **60** (2004) 91–110
16. Fischler, M.A., Bolles, R.C.: Random sample consensus: a paradigm for model fitting with applications to image analysis and automated cartography. Communications of the ACM **24** (1981) 381–95
17. Byröd, M., Josephson, K., Åström, K.: Fast and stable polynomial equation solving and its application to computer vision. Int. Journal of Computer Vision **84** (2009) 237–255

18. Kukelova, Z., Pajdla, T.: Two minimal problems for cameras with radial distortion. In: OMNIVIS. (2007)
19. Josephson, K., Byröd, M.: Pose estimation with radial distortion and unknown focal length. In: Proc. Conf. Computer Vision and Pattern Recognition, San Fransisco, USA. (2009)
20. Kukelova, Z., Bujnak, M., Pajdla, T.: Real-time solution to the absolute pose problem with unknown radial distortion and focal length. In: IEEE International Conference on Computer Vision, ICCV 2013, Sydney, Australia, December 1-8, 2013. (2013) 2816–2823
21. Hartley, R.I., Zisserman, A.: Multiple View Geometry in Computer Vision. Cambridge University Press (2000)
22. Cox, D., Little, J., O'Shea, D.: Using Algebraic Geometry. Springer Verlag (1998)
23. Cox, D., Little, J., O'Shea, D.: Ideals, Varieties, and Algorithms. Springer Verlag (2007)
24. Grayson, D., Stillman, M.: Macaulay 2. Available at http://www.math.uiuc.edu/Macaulay2/ (1993-2002) An open source computer algebra software.
25. Kuang, Y., Åström, K.: Numerically stable optimization of polynomial solvers for minimal problems. In: ECCV (3). (2012) 100–113
26. Naroditsky, O., Daniilidis, K.: Optimizing polynomial solvers for minimal geometry problems. In: ICCV. (2011) 975–982